Single-Walled Carbon Nanotube Binding Peptides: Probing Tryptophan's Importance by Unnatural Amino Acid Substitution

Zhengding Su, Kenneth Mui, Elisabeth Daub, Tong Leung, and John Honek*

Department of Chemistry, University of Waterloo, Waterloo, Ontario N2L 3G1, Canada

Received: May 24, 2007; In Final Form: October 13, 2007

Peptides selected from phage-displayed libraries have been found to exhibit high-affinity binding to carbon nanotubes including single-walled carbon nanotubes (SWNTs), multi-walled carbon nanotubes, and single-walled carbon nanohorns. One unique feature of these peptides is that their amino acid sequences are rich in tryptophan and histidine residues. The aim of this study was to investigate the importance of the tryptophan residue in a newly identified SWNT-binding peptide, UW-1, which contains the motif, *X*TH*XX*PWT*X*, where *X* is any amino acid. Tryptophan was altered in the following ways: mutation to alanine or substitution with three unnatural tryptophan analogues, i.e., 5-fluorotryptophan, 5-hydroxytryptophan, and 7-azatryptophan. Analysis of experimental and computational data suggests that the highest occupied molecular orbital of the tryptophan residue in the peptide interacts with the lowest unoccupied molecular orbital from the SWNT. This information should be important in permitting modulation of peptide affinities to these nanomaterials.

Introduction

Single-walled carbon nanotubes (SWNTs) have promising applications in the field of biotechnology and medicine due to their unique electrical, metallic, and structural characteristics.[1−4] Biomolecules interacting with SWNTs provide them with specific chemical handles that would make several of these applications possible. One of the anticipated applications of SWNTs is the noncovalent immobilization of biomolecules on the surface of SWNTs to preserve the sp^2 nanotube structure and, thus, their electronic properties. Therefore, mechanism(s) of interaction between biomolecules and SWNTs is a critical focus of investigation since the extent of nanotube functionality and reactivity in biological systems remains relatively unknown.

Structurally, SWNTs can be viewed as graphite sheets that have been rolled into seamless cylinders, resembling a single-layered planar network of interconnected hexagonal rings of carbon atoms.[5] The rings found within this network are very similar to that of a benzene ring because of conformational rigidity and planarity.[2] Attachment of proteins on the outer surface of SWNTs can be achieved by noncovalent interactions.[6] Numerous peptides have been designed or screened to bind to carbon nanotubes (CNTs). These peptides have been observed to have a strong affinity for CNTs and can be used as tools to overcome the heterogeneity and hydrophobic properties limiting the applications of CNTs.[7−12] For example, a synthetic amphiphilic alpha-helical peptide containing multiple phenylalanine residues on its hydrophobic surface has been reported to not only coat and solubilize carbon nanotubes but also control the assembly of the peptide-coated nanotubes into macromolecular structures.[7] Structure−function studies have revealed that phenylalanine plays an important role in the enhancement of peptide binding to SWNTs.[13] On the other hand, peptides obtained through screening phage-display libraries exhibit a differential high-affinity binding to certain types of nanotubes and these peptides have been found to be rich in histidine (H or His) and/or tryptophan (W or Trp) at specific locations.[14−16] Direct measurements of interactions between polylysine or polytryptophan and nanotubes have demonstrated that aromatic moieties in peptides showed stronger adhesion to nanotubes than that of polylysine.[17] These and other studies on the adsorption of polynuclear aromatic compounds to CNTs suggest that $\pi-\pi$ interactions can play a critical role in the strength of molecular contact between these compounds and nanotubes.[6,18]

Recently, we identified a SWNT-binding motif, *X*TH*XX*PWT*X*, where *X* is any amino acid, through phage-displayed peptide library screening.[15] One peptide, with the amino acid sequence of LLADTTHHRPWT (named as UW-1, Figure 1a), exhibited the highest affinity to SWNTs and formed a beta-turn structure which was induced by SWNT binding,[15] suggesting that hydrophobic interactions as well as $\pi-\pi$ interactions between the side chain of tryptophan at position 11 and the sidewalls of SWNT could play an important role in high-affinity binding. In this study, we have investigated the nature of the $\pi-\pi$ interactions between the tryptophan residue and SWNTs, using a single-point mutation as well as the incorporation of unnatural tryptophan analogs to alter the side chain properties of Trp11 in the UW-1 peptide. Their binding affinities to SWNTs were experimentally determined and further investigated utilizing computational chemistry.

Experimental Methods

Tryptophan analogs including 5-fluorotryptophan (FW), 5-hydroxytryptophan (HW), and 7-azatryptophan (AW) and single-walled carbon nanotubes (SWNTs, purity >95% catalogue no. 652512, lot no. 09310HD) were purchased from Sigma-Aldrich (Oakville, ON). The SWNTs were produced by chemical vapor deposition methods and their surfaces were not modified. The commercially available SWNTs were used directly in the experiments outlined below.

Suspension of SWNTs. The SWNTs (1 mg/mL) were suspended by sonication using a Branson Sonifier 200 sonicator (Danbury, CT) equipped with a 4 mm diameter microtip in 1× TBS buffer (50 mM Tris-HCl, 150 mM NaCl, pH 7.5)

* Corresponding author. E-mail: jhonek@uwaterloo.ca. Tel.: 519-888-4567, ext. 35817. Fax: 519-746-0435.

10.1021/jp0740301 CCC: $37.00
Published on Web 12/07/2007

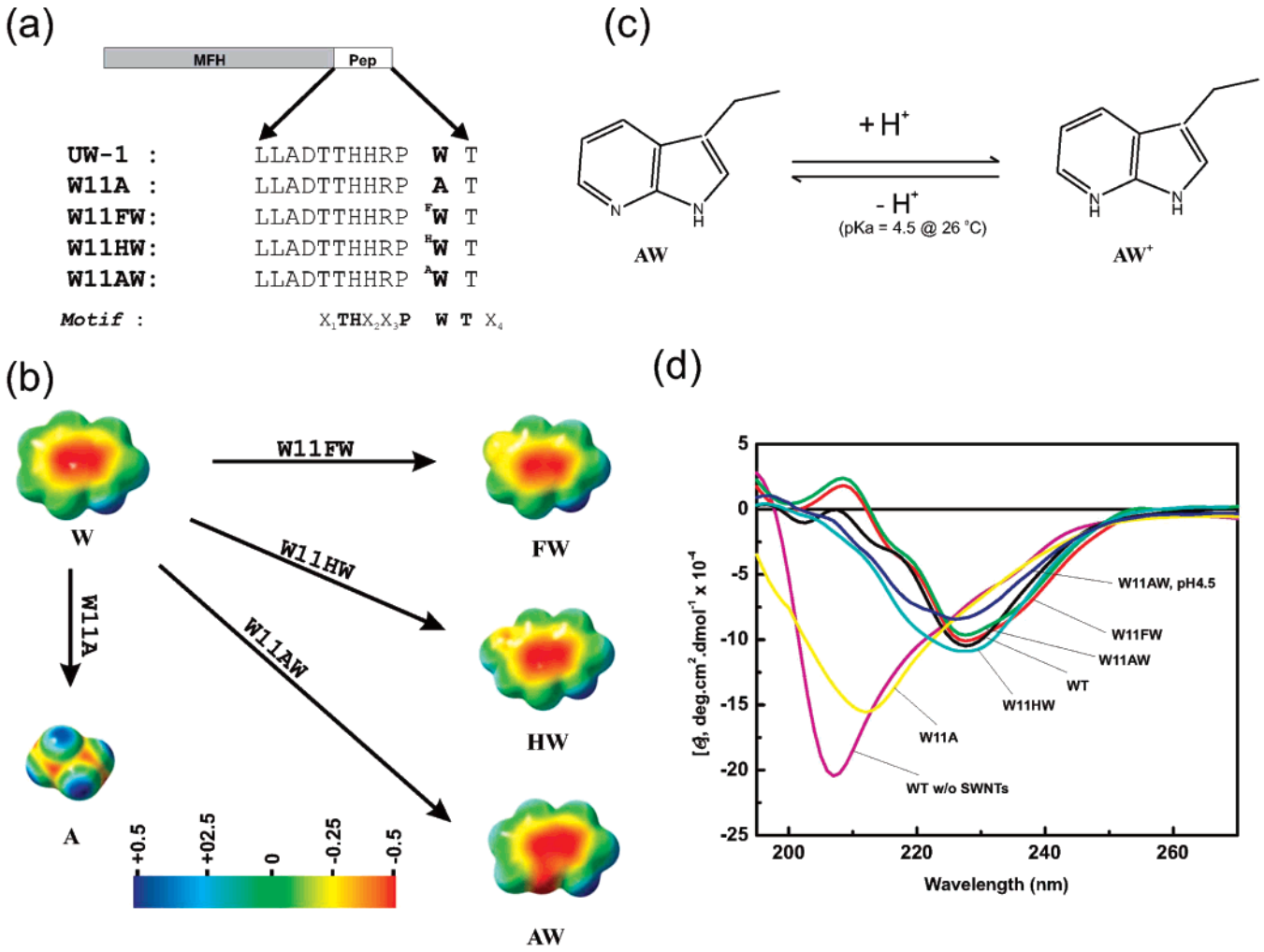

Figure 1. Amino acid sequences of the UW-1 peptide (WT) and its alanine mutant and tryptophan analog substituents. (a) MFH is a fusion carrier protein free from tryptophan and Pep is peptide. ^{F}W, ^{H}W, and ^{A}W denote 5-fluorotryptophan, 5-hydroxytryptophan, and 7-azatryptophan, respectively. (b) Comparison of indole electronic density with alanine side chain and three indole analogs calculated (AM1) and displayed using AMPAC Gui 8 (Semichem, Kansas City, MO). The unit of the scale is eV. (c) Protonation and deprotonation of AW. (d) CD spectra of UW-1 peptide and its mutants in the absence or presence of SWNTs at pH 7.5 except where indicated. Both buffer and SWNTs show insignificant CD signals (data not shown).

containing 1% Tween-20. The tip was placed into the sample approximately one-third of the distance from the surface and sonicated for 1 h with multiple 30 s bursts followed by intervals of 50 s for cooling at a power level of 13 W. When a peptide was added, the mixture was further sonicated for 2 min.

Protein Preparation. Construction of the fusion protein expression vector containing a single copy of the gene for the UW-1 peptide was prepared with a recombinant DNA approach described previously.[19] The fusion carrier protein does not contain tryptophan residues and only one tryptophan in the expressed fusion is located at position 11 in the UW-1 peptide (Figure 1a).[15] Mutation of the tryptophan 11 of the UW-1 peptide to alanine was performed by standard PCR methods as reported previously.[15]

Fusion proteins of the wild type (WT) and the alanine mutant (W11A) were prepared by transforming the particular plasmids into *Escherichia coli* BL21 (*DE3*) as the host strain. An overnight culture (50 mL) grown in LB containing ampicillin (100 μg/mL) was used to inoculate 1 L of LB medium supplemented with ampicillin (100 μg/mL). Incorporation of three tryptophan analogs, FW, HW, and AW, was accomplished with a Trp auxotrophic *E. coli* strain (W3110)[20] and expressed in M9 medium with the addition of each analog (20−40 mg/L). The cells were grown at 37 °C to a density of OD_{600nm} = 0.8 and induced by adding isopropyl β-D-1-thiogalactopyranoside (IPTG) to a final concentration of 1 mM. The induced cells were incubated for 12 h at 37 °C and collected by centrifugation ($\times$5000*g* for 30 min). The cell pellet was frozen at −20 °C before further processing.

Thawed cell pellets were resuspended in a lysis buffer (6 M urea, 50 mM phosphate, pH 8.0, 100 mM NaCl) by gentle shaking for 20 min and then sonicated for 1 min on ice. The lysis mixture was then centrifuged at 10000 rpm for 30 min and the supernatant was subjected to purification by a fast flow Ni-nitrilotriacetic acid (Ni-NTA) affinity column (Qiagen, Mississauga ON) under denaturing conditions. Simply, the supernatant of the cell lysate was loaded onto a column equilibrated with the lysis buffer. The column was extensively washed with the lysis buffer containing 50 mM imidazole, and this was followed by elution of the fusion proteins utilizing the lysis buffer containing 250 mM imidazole. The eluent was desalted using a Waters Sep-Pak C_{18} column (Mississauga, ON) and eluted with 50% acetonitrile and 0.1% TFA. The protein solution was lyophilized to dryness.

Binding Assay. Binding assays were performed according to previously reported protocols.[15] Binding affinity of fusion proteins to SWNTs was quantified by measuring the amount of protein (or peptide) binding to SWNTs. The fusion protein

TABLE 1: Binding Affinities of the Wild-Type Protein and Its Mutant and Tryptophan Analog Substituents[a]

fusion protein	incorporation efficiency (%)	relative binding affinity (%)	pH
WT		100	7.0
W11A		38 ± 8	7.0
W11FW	96	77 ± 12	7.0
W11HW	97	253 ± 32	7.0
W11AW	93	45 ± 8	7.0
W11AW$^+$	93	27 ± 6	5.0

[a] Note: The affinity was expressed as the percentage of the WT (100%). AW$^+$ denotes protonated 7-azatryptophan.

was incubated with SWNTs and washed with TBS buffer containing 0.1−0.3% Tween-20 until the OD_{280nm} in the washing solution did not decrease. Bound proteins were eluted with the acid elution buffer (2 M glycine-HCl, pH 2.2) and protein concentrations were determined with the predicted extinction coefficient for each fusion protein.[21] The determined extinction coefficients for the proteins examined were as follows: 16083.6 M^{-1} cm^{-1} for WT, 10430 M^{-1} cm^{-1} for W11A, 15930 M^{-1} cm^{-1} for W11FW, 15260 M^{-1} cm^{-1} for W11HW, and 16400 M^{-1} cm^{-1} for W11AW. Each point is the average value from five independent experiments.

Circular Dichroism. Circular dichroism (CD) was performed on free peptides in solution or in the presence of SWNTs using a Jasco J-715 spectropolarimeter (Easton, MD). Peptides were dissolved in TBS buffer (pH7.5) at a concentration of 6−20 μM. The spectra were measured between 195 and 270 nm as the average of ten successive scans with a bandwidth of 1.0 nm and a scan speed of 20 nm/min.

Raman Spectroscopy. Raman spectra were recorded using a Renishaw 1000 Raman system with cooled CCD detector (New Mills, UK). Excitation was achieved using the 632.8 nm (~1.96 eV) line of a Melles Griot 33 mW helium−neon laser, which is in resonance with both metallic and semiconducting SWNTs.[8] Samples for Raman analysis were prepared as follows: the final SWNT supernatant (~2 μL) was spotted on a glass slide and allowed to dry in a desiccator overnight prior to Raman analysis. The laser power at the samples was about 10% of that from the laser source and focused to ~1 μm. Wavenumber calibration was done using the 520.5 cm^{-1} line of a silicon wafer. The spectra of pelleted SWNTs were recorded by scanning the 70−500 cm^{-1} region (15 times) and 500−2000 cm^{-1} region (5 times) with a time constant of 20 ms.

Assignments of individual peaks in the Raman RBM region were based on the following expression,

$$\bar{v} = A/d_t + B$$

where d_t is the diameter of the nanotube (nm). Parameters A and B are equal to 223.5 and 12.5, respectively.[22]

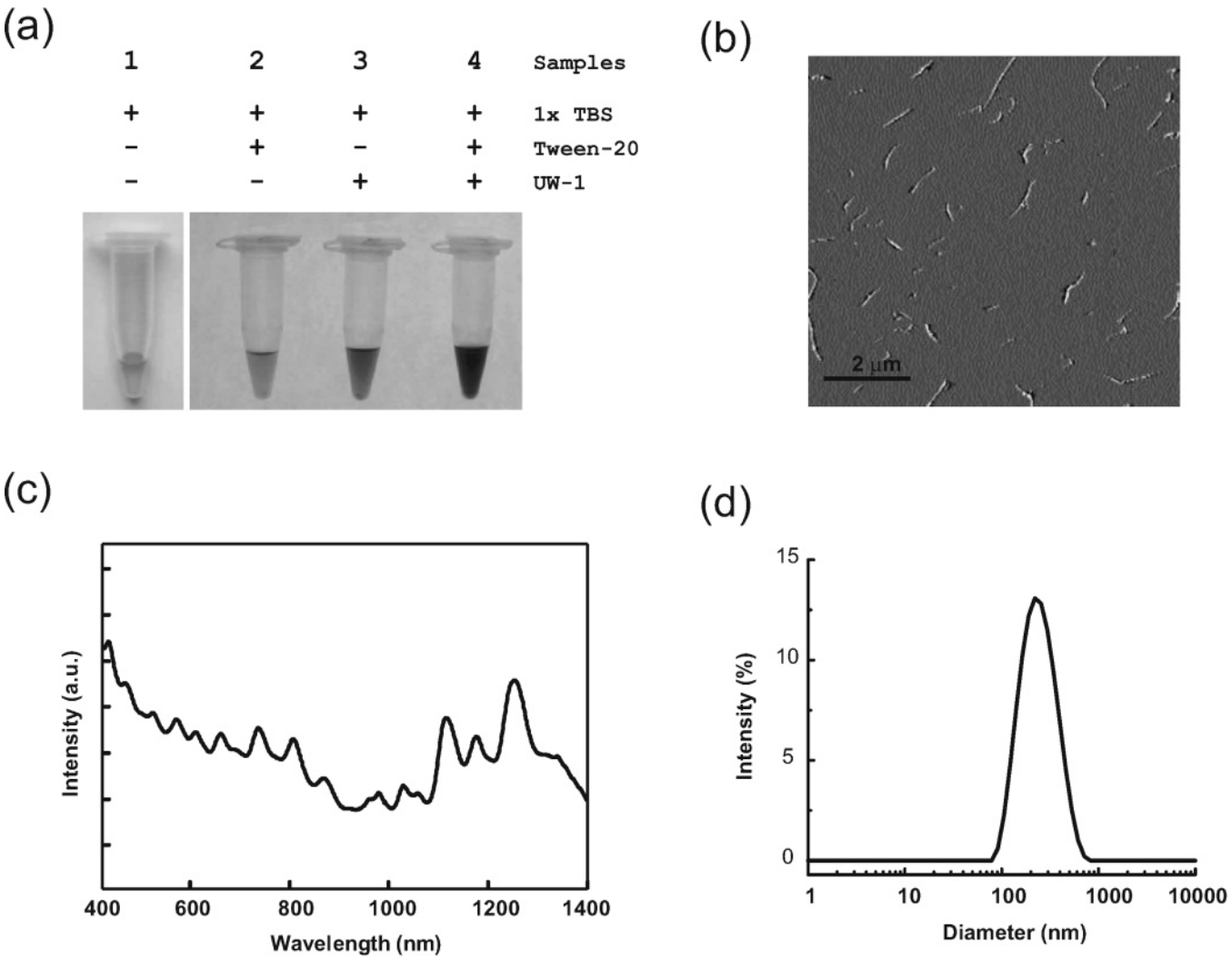

Figure 2. Solubility enhancement of SWNTs by the UW-1 peptide. (a) Photographs of vials showing sonicated SWNTs in 1× TBS buffer in the absence or presence of 1% Tween-20 and/or the UW-1 peptide. (b) AFM image of SWNTs suspended by the UW-1 peptide. (c) UV−vis−NIR absorption spectra of SWNTs in the presence of UW-1 peptide. (d) Size distribution of the UW-1 peptide suspended SWNTs as revealed by DLS.

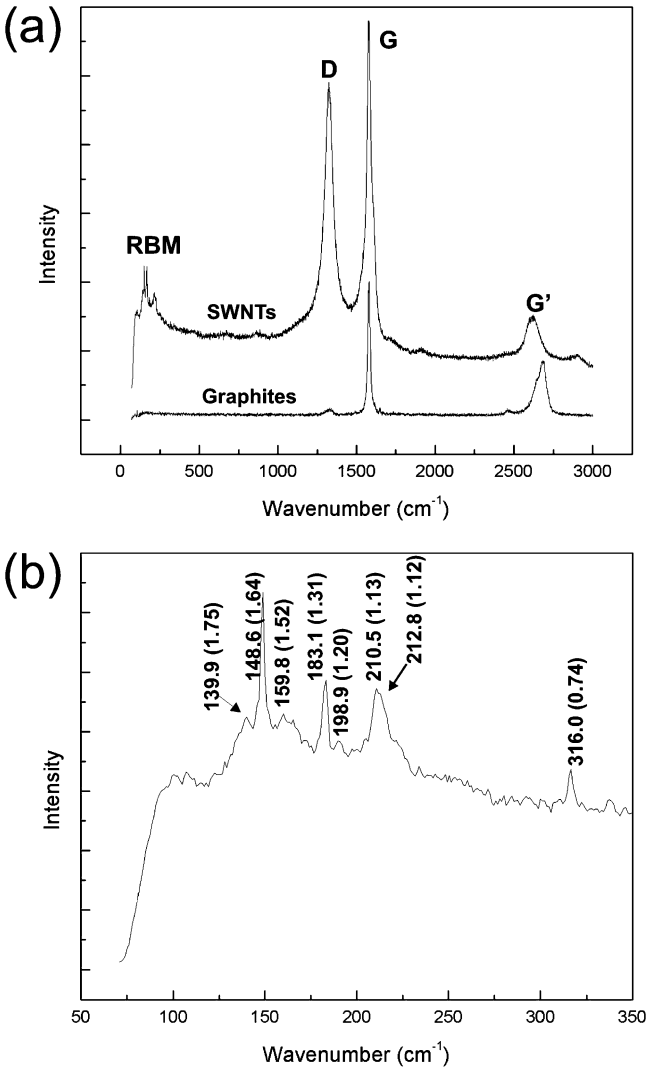

Figure 3. Characterization of the SWNTs by Raman spectroscopy. (a) A whole spectrum of the SWNTs was recorded and compared with that of spectra obtained on graphite. RBM denotes "radial breath mode". (b). Raman RBM regions of the SWNTs. Some major peaks are indicated in the panel with corresponding diameters of SWNTs in parentheses (see context for detailed calculation).

Atomic Force Microscopy (AFM). The aforementioned SWNT pellets were suspended in H_2O with a short sonication time (~10 s). Immediately, 10 μL volumes were dropped onto clean silicon substrates under ambient conditions and dried at 37 °C in a vacuum oven. AFM studies were carried out in tapping mode using a Digital Instruments Dimension 3100 Atomic Force Microscope (Veeco, Woodbury, NY).

UV/Vis/NIR Spectroscopy. The absorption spectrum of SWNTs suspended by peptide was obtained using a Varian Cary 5000 UV−vis−NIR spectrophotometer.

Dynamic Light Scattering (DLS). DLS measurements of the average d_s and μ values were obtained using a Malvern Zetasizer Nano instrument (Brookhaven Instruments, Holtsville, NY) at 25 °C. Sample solutions contained 5×10^{11} particles/mL, 1 × TBS buffer, and 1% (w/v) Tween-20. A scattering angle of 90° was used for the DLS measurements of particle size, and the results are reported as the average and standard deviation from more than five DLS measurements.

Computational Modeling. All structures were drawn and visualized using SPARTAN '06 for Windows (Version 1.0.2; Wavefunction Inc., Irvine, CA). Geometry optimizations and frequency calculations were performed using five selected methods (i.e., AM1, RHF/3-21G, RHF/6-31G*, B3LYP/6-31G*, and MP2/6-31G*) using default conditions in SPARTAN. All frequency calculations for Trp and its analogs yielded no negative frequencies, indicating all structures used for highest occupied molecular orbital (HOMO) and lowest unoccupied molecular orbital (LUMO) energy calculations were energy minima.[23]

Results and Discussion

Site-directed mutagenesis was utilized to generate an MFH-UW-1 fusion peptide analog that contained alanine in place of the tryptophan (i.e., W11A where 11 refers to tryptophan-11 in the UW-1 peptide that interacts with SWNTs) (Figure 1a; see Experimental Methods). This mutation was utilized to probe the importance of the tryptophan residue in the interaction between the UW-1 peptide and SWNTs. The Trp→Ala mutation produces a large reduction of the side-chain size and the elimination of its aromatic character. To probe the electronic and orbital contributions of Trp, the substitution of tryptophan by tryptophan analogs included FW, HW, and AW and was performed through in vivo incorporation (see Experimental Methods). In principle, such analogs will generate an electron-withdrawing effect in the case of FW as well as an electron-donating effect in the case of HW with respect to their aromatic side chains (Figure 1b). The effect of AW on this donor−acceptor interaction would be dependent upon its environment (e.g., the solution pH value, see Figure 1c). As a result, these variations should reveal in detail the critical parameters in the structure of tryptophan that are pertinent to the UW-1/SWNT interaction. The incorporation efficiency of the three tryptophan analogs at position 11 of the UW-1 peptide was analyzed and confirmed to be ≥93% for each analog using electrospray mass spectrometry, absorption, and fluorescence spectroscopic techniques, according to methods described previously by Mohammadi et al.,[24] Broos et al.,[25] and Senear et al.[26] (see Supporting Information). Detailed data for individual incorporation efficiencies are listed in Table 1. Previously, we found that the UW-1 peptide exhibits a beta-hairpin conformation induced by binding to SWNTs.[15] In the absence of SWNTs, all mutant peptides (i.e., W11A, W11FW, W11HW, and W11AW) exhibit extended conformations similar to that of WT (Figure 1d). In the bound state with SWNTs, substitution of Trp11 by Ala can dramatically alter the conformation of peptide, while replacement of Trp11 with tryptophan analogs (i.e., FW, HW, and AW in this case) does not significantly affect peptide conformation (Figure 1d).

SWNT suspensions were prepared in 1× TBS buffer (50 mM Tris-HCl, pH 7.5, 150 mM NaCl) containing 1% Tween-20 by sonication and were clarified by centrifugation. The as-purified SWNTs in solution showed no visible signs of precipitation over a 2-week period (sample 2 in Figure 2a). Raman spectra were collected for the as-purified SWNTs deposited on glass slides. By comparison, graphite spectra were collected in the same method. As shown in Figure 3a, one Raman spectrum exhibited typical absorbance bands in the radial breathing mode (RBM) range, D, G, and G′ bands. Apparently, the current as-purified SWNTs utilized in this study contain different types of SWNTs including metallic and semiconductive tubes as the intensities of the **D** and **G** bands are relevant to the population of nanotube modes.[27] Furthermore, these RBM data indicate that the diameters of the suspended SWNTs are in the range from 1.12 to 1.75 nm (Figure 3b), calculated based on the wavenumber data.

TABLE 2: Calculated Energy Levels of Tryptophan and Its Analogs (kJ/mol)

	AM1		RHF/3-21G		RHF/6-31G*		B3LYP/6-31G*		MP2/6-31G*
	HOMO	LUMO	HOMO	LUMO	HOMO	LUMO	HOMO	LUMO	HOMO	LUMO
W	−810.8	28.95	−750.98	359.34	−733.46	362.94	−521.04	−6.32	−721.3	348.44
FW	−830.5	0.8766	−785.59	319.35	−762.87	328.22	−540.24	−32.05	−754.37	312.43
HW	−800.9	14.89	−742.68	341.8	−727.23	346.99	−500.36	−11.78	−727.01	331.09
AW	−847.2	4.78	−794.76	313.03	−771.99	314.29	−561.88	−59.2	−754.74	295.47
AW^+	−1302	−518.7	−1287.87	−256	−1267.38	−245.29	−1048.15	−610.08	−1239.09	−255.49
higher	HW	W	HW	W	HW	W	HW	W	W	W
	W	HW	W	HW	W	HW	W	HW	HW	HW
↓	FW	FW	FW	FW	FW	FW	FW	FW	FW	FW
↓	AW	AW	AW	AW	AW	AW	AW	AW	AW	AW
lower	AW^+	AW^+	AW^+	AW^+	AW^+	AW^+	AW^+	AW^+	AW^+	AW^+

The UW-1 peptide can significantly enhance the solubility of the SWNTs in the absence or in the presence of Tween-20 (i.e., samples 3 and 4, respectively, in Figure 2a). This is supported by an AFM image of 0.1 mg/mL SWNTs in solution, which were formed in a thin film on a silicon wafer, showing well-dispersed SWNTs (Figure 2b). The optical absorption spectrum of the peptide-mediated suspension of SWNTs shows multiple well-defined peaks from visible to NIR regions (Figure 2c). These peaks represent optical transitions between singularities for a specific type of tube (n,m) and are evidence that the UW-I peptide efficiently debundles SWNTs, in combination with sonication. Furthermore, DLS experiments indicated that the statistical distribution of the length of the solubilized SWNTs was approximately 200−500 nm (Figure 2c), which is consistent with the data provided by the supplier. Taken together, these data suggest that the UW-1 peptide can disperse and stabilize SWNTs in aqueous solution.

Table 1 also summarizes the binding affinities of the UW-1 mutants to the SWNTs, which are expressed as percentages to that of the WT protein (i.e., the UW-1 peptide). These values have been calibrated with their incorporation efficiency of tryptophan analogs. Notably, at neutral pH, mutation of Trp11 to Ala (i.e., W11A) dramatically reduced binding affinity as much as 62% compared with that of WT, indicating that Trp11 plays a key role in the binding of the UW-1 peptide to the SWNTs. On the other hand, peptides containing the tryptophan analogs exhibited distinct and different effects on the binding affinities of the UW-1 peptide to the SWNTs. The mutant W11FW reduced binding affinity by as much as 23%, while the mutant W11HW enhanced binding affinity of the peptide by 2.5-fold. As expected, the binding affinity of the mutant W11AW to the SWNTs was pH-dependent. At neutral pH or below (e.g., pH 5.0) (note that the pK_a value for the side chain of AW is 4.5 at 26 °C[28]), the binding affinity of the peptide decreased. Taken together, the order of binding affinity for the UW-1 peptide and its analogs is as follows: W11HW > WT > W11FW > W11AW > $W11AW^+$, where AW^+ represents the protonated form of 7-azatryptophan.

We next questioned the nature of the possible orbital mixing/charge-transfer interactions which might contribute to the binding of the tryptophan side chain with SWNTs. Considering the general nature of the chemisorptive interaction involved in $\pi-\pi$ stacking,[29−31] the distinct binding affinities of different Trp analogs suggest that some structure-dependent aspects of the interactions might be correlated with electron donor or acceptor properties. The absorptive adducts might be expected to occur by a face-to-face interaction, common for $\pi-\pi$ interactions.[18] However, even if this interaction is accompanied by an electron donor−acceptor charge-transfer interaction between the aromatic adsorbate and the aromatic sidewalls of the SWNT, it would be difficult to predict which Trp analog would produce a more favorable interaction with the SWNT because the electrochemical properties of the sidewalls of SWNTs are not yet fully understood.[32] Therefore, electronic structure calculations were undertaken to analyze the energy levels of each Trp analog side chain with respect to their lowest unoccupied molecular orbital (LUMO) and their highest occupied molecular orbital (HOMO) using several electronic calculation methods (AM1, RHF/3-21G, RHF/6-31G*, B3LYP/6-31G*, and MP2/6-31G*) as incorporated in SPARTAN'06 (Wavefunction Inc., Irvine, CA) to determine if there is a correlation between either of these energies and the experimental trends observed for these interactions (see Experimental Methods for details). The calculation results, based on the selected methods, are summarized in Table 2. As depicted in Table 2, the energy levels of the LUMO and the HOMO orbitals for each analog are ranked from higher to lower. In all the considered methods except MP2/6-31G*, the HOMO energies are ranked in the same order, i.e., HW > W > FW > AW > AW^+. This order is consistent with that of the observed peptide

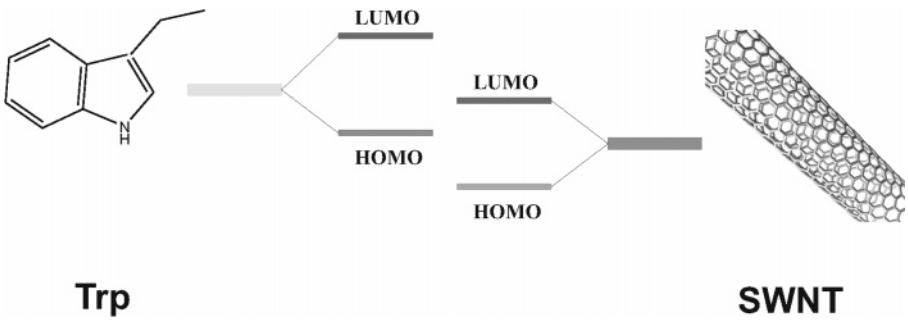

Figure 4. Mechanism of electron donor−acceptor interactions between the trytophan side chain and the sidewall of a SWNT, where LUMO, the lowest unoccupied molecular orbital, and the HOMO, the highest occupied molecular orbital, are shown. This scheme was based on a comparison of the binding affinities of different peptides to SWNTs as well as computational modeling. It is highly likely that the interaction of tryptophan and the SWNT results from orbital mixing between the HOMO of the tryptophan side chain and the LUMO of SWNT.

binding affinities (see Table 1). In fact, in the MP2/6-31G* mode, both HOMO energy levels of 5HW and W are close to each other. By contrast, all the LUMO data are in the order of W > HW > FW > AW > AW^+ for all five selected computational methods, which is inconsistent with the observed binding affinities. Based on the experimental results listed in Table 1, the relative differences of the energy levels of the tryptophan side chains and the sidewall of a SWNT can be depicted as shown in Figure 4. As a result, these data suggest that it is likely that the orbital mixing in the $\pi-\pi$ interaction takes place between the HOMO of the tryptophan and the LUMO of the sidewall of the SWNT, implying that the sidewall of SWNTs acts in this instance as an electron acceptor and the indole ring as an electron donor.

Previous analysis on the interaction of SWNTs with anthracene derivatives reported by Zhang et al.[18] suggested that, in that specific type of interaction, the SWNT acts as the electron donor and the anthracene as electron acceptor. As a result, electron-withdrawing substituents on the anthracenes were observed to bind more strongly. If the tryptophan analogs in this work behaved in a similar fashion, one would predict that the binding affinities of the peptides would follow an order from stronger to weaker: $W11AW^+$ > W11AW > W11FW > WT > W11HW. This predicted order is opposite that obtained from our experimental data. A recent theoretical study by Lu et al. has revealed that molecular size and orientation play critical roles in the selective interaction of large or charge-transfer aromatic molecules with metallic SWNTs.[33] In their report, benzene showed no selective interaction with SWNTs. However, when phenylalanine is arranged in repeating peptide segments, it has been shown that phenylalanine residues can function as anchors to wrap SWNTs.[9,13] Although we cannot exclude the possibility that peptide conformational change may affect binding affinity, it is highly likely that Trp11 in the UW-1 peptide plays a critical role in both maintaining peptide conformation and anchoring the peptide on the SWNT surface. Very recently, De Miranda and Walsh used an existing polarizable force field to model the interactions between SWNTs and peptides, supporting the fact that the aromatic side chains of histidine and tryptophan are key factors in specific binding to SWNTs.[34] Taken together, our study and others suggest that SWNTs can be either electron donors or acceptors in these types of interactions.

Conclusion

In summary, we have analyzed the importance of tryptophan residues in the molecular interaction of a phage-displayed peptide with SWNTs. The $\pi-\pi$ interaction between the tryptophan side chain in the UW-1 peptide and the sidewall of SWNT is a major factor for physisorption, which appears to be dependent upon the orbital interactions between the highest occupied molecular orbital (HOMO) of the tryptophan indole ring and the lowest unoccupied molecular orbital (LUMO) of the SWNT. Our new finding should have important implications for understanding and designing SWNT surfaces of biological significance, and for the application of designed peptides in the purification and assembly of SWNTs. Moreover, this could lead to the immobilization of peptide-attached SWNTs on substrate surfaces, a promising way to arrange nanotubes into architectures useful for electrical circuits and molecular sensing applications. The control of peptide affinity to SWNTs by selection of the appropriate tryptophan side chain could allow for fine-tuning of this type of interaction in terms of strength and pH (e.g., with 7-azatryptophan). It is important to note that there are diverse solutions in nature to molecular recognition of xenomaterials such as SWNTs that depend on sequence as well as conformation of the biomolecule.

Acknowledgment. We thank NSERC Nano-IP for financial support of this research, Dr. Guy Guillemette for the auxotrophic strain (*E. coli* W3110) utilized in this study, and Randy Fagan, Zhenhua He, and Nicole Sukdeo for their technical assistance and Dr. Michael Collins for allowing us to use the UV−vis−NIR spectrophotometer.

Supporting Information Available: The incorporation of tryptophan analogs in peptide samples as characterized by absorbance and fluorescence spectroscopy and mass spectrometry. This material is available free of charge via the Internet at http://pubs.acs.org.

References and Notes

(1) Bianco, A.; Kostarelos, K.; Prato, M. *Curr. Opin. Chem. Biol.* **2005**, *9*, 674−679.
(2) Martin, C. R.; Kohli, P. *Nat. Rev. Drug Discovery* **2003**, *2*, 29−37.
(3) Li, J.; Ng, H. T.; Chen, H. *Methods Mol. Biol.* **2005**, *300*, 191−223.
(4) Contarino, M. R.; Sergi, M.; Harrington, A. E.; Lazareck, A.; Xu, J.; Chaiken, I. *J. Mol. Recognit.* **2006**, *19*, 363−371.
(5) Iijima, S. *Nature* **1991**, *354*, 56−58.
(6) Chen, R. J.; Zhang, Y.; Wang, D.; Dai, H. *J. Am. Chem. Soc.* **2001**, *123*, 3838−3839.
(7) Dieckmann, G. R.; Dalton, A. B.; Johnson, P. A.; Razal, J.; Chen, J.; Giordano, G. M.; Munoz, E.; Musselman, I. H.; Baughman, R. H.; Draper, R. K. *J Am. Chem. Soc.* **2003**, *125*, 1770−1777.
(8) Ortiz-Acevedo, A.; Xie, H.; Zorbas, V.; Sampson, W. M.; Dalton, A. B.; Baughman, R. H.; Draper, R. K.; Musselman, I. H.; Dieckmann, G. R. *J Am. Chem. Soc.* **2005**, *127*, 9512−9517.
(9) Zorbas, V.; Ortiz-Acevedo, A.; Dalton, A. B.; Yoshida, M. M.; Dieckmann, G. R.; Draper, R. K.; Baughman, R. H.; Jose-Yacaman, M.; Musselman, I. H. *J Am. Chem. Soc.* **2004**, *126*, 7222−7227.
(10) Karajanagi, S. S.; Yang, H.; Asuri, P.; Sellitto, E.; Dordick, J. S.; Kane, R. S. *Langmuir* **2006**, *22*, 1392−1395.
(11) Pender, M. J.; Sowards, L. A.; Hartgerink, J. D.; Stone, M. O.; Naik, R. R. *Nano Lett.* **2006**, *6*, 40−44.
(12) Bianco, A.; Hoebeke, J.; Kostarelos, K.; Prato, M.; Partidos, C. D. *Curr. Drug Deliv.* **2005**, *2*, 253−259.
(13) Zorbas, V.; Smith, A. L.; Xie, H.; Ortiz-Acevedo, A.; Dalton, A. B.; Dieckmann, G. R.; Draper, R. K.; Baughman, R. H.; Musselman, I. H. *J. Am. Chem. Soc.* **2005**, *127*, 12323−12328.
(14) Kase, D.; Kulp, J. L., III; Yudasaka, M.; Evans, J. S.; Iijima, S.; Shiba, K. *Langmuir* **2004**, *20*, 8939−8941.
(15) Su, Z.; Leung, T.; Honek, J. F. *J. Phys. Chem. B* **2006**, *110*, 23623−23627.
(16) Wang, S.; Humphreys, E. S.; Chung, S. Y.; Delduco, D. F.; Lustig, S. R.; Wang, H.; Parker, K. N.; Rizzo, N. W.; Subramoney, S.; Chiang, Y. M.; Jagota, A. *Nat. Mater.* **2003**, *2*, 196−200.
(17) Li, X.; Chen, W.; Zhan, Q.; Dai, L.; Sowards, L.; Pender, M.; Naik, R. R. *J. Phys. Chem. B* **2006**, *110*, 12621−12625.
(18) Zhang, J.; Lee, J. K.; Wu, Y.; Murray, R. W. *Nano Lett.* **2003**, *3*, 403−407.
(19) Su, Z.; Vinogradova, A.; Koutychenko, A.; Tolkatchev, D.; Ni, F. *Protein Eng. Des. Sel.* **2004**, *17*, 647−657.
(20) Bachmann, B. J. *Microbiol. Rev.* **1983**, *47*, 180−230.
(21) Gill, S. C.; von Hippel, P. H. *Anal. Biochem.* **1989**, *182*, 319−326.
(22) Bachilo, S. M.; Strano, M. S.; Kittrell, C.; Hauge, R. H.; Smalley, R. E.; Weisman, R. B. *Science* **2002**, *298*, 2361−2366.
(23) Anslyn, E. V.; Dougherty, D. A. *Modern Physical Orgnaic Chemistry*; University Science Books: Savsalito, CA, 2006; p 1099.
(24) Mohammadi, F.; Prentice, G. A.; Merrill, A. R. *Biochemistry* **2001**, *40*, 10273−10283.
(25) Broos, J.; Gabellieri, E.; Biemans-Oldehinkel, E.; Strambini, G. B. *Protein Sci.* **2003**, *12*, 1991−2000.
(26) Senear, D. F.; Mendelson, R. A.; Stone, D. B.; Luck, L. A.; Rusinova, E.; Ross, J. B. *Anal. Biochem.* **2002**, *300*, 77−86.
(27) Dresselhaus, M. S.; Dresselhaus, G.; Saito, R.; Jorio, A. *Phys. Rep.* **2005**, *409*, 47−99.
(28) Chen, Y.; Rich, R. L.; Gai, F.; Petrich, J. W. *J. Phys. Chem.* **1993**, *97*, 1770−1780.

(29) Tauer, T. P.; Sherrill, C. D. *J. Phys. Chem. A* **2005**, *109*, 10475−10478.
(30) Hobza, P.; Selzle, H. L.; Schlag, E. W. *J. Am. Chem. Soc.* **1994**, *116*, 3500−3506.
(31) Sinnokrot, M. O.; Valeev, E. F.; Sherrill, C. D. *J. Am. Chem. Soc.* **2002**, *124*, 10887−10893.
(32) Ouyang, M.; Huang, J. L.; Lieber, C. M. *Acc. Chem. Res.* **2002**, *35*, 1018−1025.
(33) Lu, J.; Nagase, S.; Zhang, X.; Wang, D.; Ni, M.; Maeda, Y.; Wakahara, T.; Nakahodo, T.; Tsuchiya, T.; Akasaka, T.; Gao, Z.; Yu, D.; Ye, H.; Mei, W. N.; Zhou, Y. *J. Am. Chem. Soc.* **2006**, *128*, 5114−5118.
(34) De Miranda, S.; Walsh, T. R. *Mol. Phys.* **2007**, *105*, 221−229.